

CONTRAST FEATURES OF BREAST CANCER IN FREQUENCY-DOMAIN LASER SCANNING MAMMOGRAPHY

K. Thomas Moesta,[†] Sergio Fantini,[‡] Helge Jess,* Susan Totkas,[†] Maria A. Franceschini,[‡] Michael Kaschke,* and Peter M. Schlag[†]

[†]Humboldt University, Robert Roessle Hospital and Tumor Institute at the Max Delbrueck Center for Molecular Medicine, Virchow-Charité, 13122 Berlin, Germany; [‡]University of Illinois at Urbana Champaign, Laboratory for Fluorescence Dynamics, Department of Physics, Illinois; *Carl Zeiss, Oberkochen, Germany

(JBO/NIR-24 received Nov. 30, 1996; revised manuscript received Aug. 10, 1997; accepted for publication Sep. 7, 1997.)

ABSTRACT

Frequency-domain optical mammography has been advocated to improve contrast and thus cancer detectability in breast transillumination. To the best of our knowledge, this report provides the first systematic clinical results of a frequency-domain laser scanning mammograph (FLM). The instrument provides monochromatic light at 690 and 810 nm, whose intensity is modulated at 110.0010 and 110.0008 MHz, respectively. The breast is scanned by stepwise positioning of source and detector, and amplitude and phase for both wavelengths are measured by a photomultiplier tube using heterodyne detection. Images are formed representing amplitude or phase data on linear gray scales. Furthermore, various algorithms carrying on more than one signal (amplitude ratio, phase difference, μ_a , μ_s' , N) were essayed. Twenty visible cancers out of 25 cancers in the first 59 investigations were analyzed for their quantitative contrast with respect to the whole breast or to defined reference areas. Contrast definitions refer to the signal itself (definition 1), to the signal noise (definition 2), or were based on nonparametric comparison (definition 3). The amplitude signal provides better contrast than the phase signal. Ratio images between red and infrared amplitudes gave variable results; in some cases the tumor contrast was canceled. The algorithms to determine μ_a and μ_s' from amplitude and phase data did not significantly improve upon objective contrast. The N algorithm, using the phase signal to flatten the amplitude signal did significantly improve upon contrast according to contrast definitions 1 and 2, however, did not improve upon nonparametric contrast. Thus, with the current instrumentation, the phase signal is helpful to correct for the complex and variable geometry of the breast. However, an independent informational content for tumor differentiation could not be determined. The flat field algorithm did greatly enhance optical contrast in comparison with amplitude or amplitude ratio images. Further evaluation of FLM will have to be based on the N -algorithm images. © 1998 Society of Photo-Optical Instrumentation Engineers.

[S1083-3668(98)00202-0]

Keywords laser; breast neoplasm's diagnosis; near infrared imaging.

1 INTRODUCTION

Conventional transillumination of the breast has been shown to be inferior to x-ray mammography in terms of sensitivity and specificity.^{1–6} Contrast improvement has been proposed by the determination of the time a photon had traveled within the tissue prior to contributing to an image. This time determination can be accomplished either by direct time-of-flight measurements after short light pulses (time-domain approach) or by phase detection of intensity modulated light^{7–9} (frequency-domain approach). The frequency domain approach offers an

economic advantage and an improved signal to noise ratio by using the entire amount of light exiting the breast instead of just a small subset of early photons as in time domain techniques based on time gating. We have demonstrated clinical feasibility of frequency-domain laser scanning transmission mammography (FLM), using a first clinical prototype of such instrument developed by Zeiss, Oberkochen. We have also developed an algorithm for edge effect corrections based on the phase information obtained.¹⁰ It is the purpose of the present work to quantitatively analyze the quality of contrast which is obtained for invasive cancers by various imaging modalities and algorithms.

Address all correspondence to K. Thomas Moesta, Robert Roessle Hospital, Humboldt University, Lindenberger Weg 80, 13122 Berlin, Germany; Tel: 49 30 9417 1400/1426; Fax: 49 30 9417 1499.

2. MATERIAL AND METHODS

2.1 INSTRUMENTATION

A frequency-domain dual wavelength laser scanning mammograph (FLM) has been developed at Carl Zeiss, Oberkochen under the name LIMA (*Licht Mammograph*). The light sources are sinusoidally modulated at frequencies $f_{\text{Red}}=110.0010$ MHz and $f_{\text{IR}}=110.0008$ MHz. The mean light power is adapted to the optical density of the breast with a maximum value of 10 mW. All electrical and electronic components are located in a rack physically separated from the patient, and the light is delivered to the breast via glass fibers. The light is there collimated and projected onto one side of the breast as a 2 mm diameter incident beam. The breast is positioned between two parallel glass plates, which are approached until the patient perceives discomfort. The incident beam is scanned over one side of the breast, while the aperture of a fiber bundle with 5 mm in diameter is scanned in tandem over the opposite side. The detector consists of a photomultiplier tube (PMT) whose gain is modulated at $f=110$ MHz. The resulting cross-correlation frequencies are $df_{\text{Red}}=1$ kHz and $df_{\text{IR}}=0.8$ kHz, and they carry the phase and amplitude informations at λ_{Red} and λ_{IR} , respectively. Further signal processing used lock-in amplification or digital data processing. For mechanical reasons the setup of the first instrument used in this study did not enable us to investigate the portion of the breast at distances smaller than approximately 2 cm from the chest wall. Detailed descriptions of the instrument have been communicated elsewhere.^{10,11}

2.2 IMAGES

Images were stored as separate data matrices of phase and amplitude signal for both wavelengths. Images of the amplitude (ac image) and phase were obtained by projecting the data on linear gray or color scales. Additional processing used the commercial software package TRANSFORM (Spyglass) to allow for gray scale adaptations. Algorithms requiring two data sets (either amplitude and phase, or both wavelengths) were programmed in PASCAL and implemented into a semi-automatic software for clinical data analysis.

2.1.1 Ratios and Differences

The amplitude ratios $\Psi_{\text{AC}}^{\text{Red}}/\Psi_{\text{AC}}^{\text{IR}}$ or the phase differences $\varphi_{\text{Red}}-\varphi_{\text{IR}}$ were calculated and represented on linear gray scales, as described above.

2.1.2 Edge Effect Correction—the N image

Towards the edge of the breast, two phenomena will superimpose to the intrinsic variations in absorption: the boundary photon losses, reducing the amount of photons transmitted to the detector and, of major significance, the reduction in breast thickness, which increases the signal transmitted. The

dynamic range of the amplitude signal is governed by those edge effects and, if the data is represented on a linear gray scale, smaller signal perturbations cannot yield sufficient contrast.

Based on the observation that the phase signal is linearly dependent on the geometrical breast thickness along the source-detector line and is not significantly affected by photon losses at the boundary, we developed a calculated parameter, called $N(x,y)$, which represents the amplitude signal corrected for edge effects.^{10,11}

2.1.3 Images of μ_a and μ_s

Under the assumption that within the sampled volume at pixel (x,y) the tissue optical parameters $\mu_a=\langle\mu_a\rangle$ and $\mu_s'=\langle\mu_s'\rangle$ are constant, the local tissue optical parameters can be determined directly from the raw data as described in Reference 12.

2.3 PATIENTS

Twenty patients with invasive breast cancers visible in both perpendicular views of FLM in any of the above described images were selected from the first 59 consecutive investigations. In that series, five invasive cancers did not show a corresponding inhomogeneity in the two perpendicular views, two patients had noninvasive cancers, 16 patients had benign disease, and 16 investigations were unevaluable. The reasons for unevaluability were technical in five cases, geometrical (tumor very close to the chest wall, not enclosed in the FLM specific field of view) in five cases, a lack of definitive histology (patients not operated upon after complete diagnostic assessment) in three cases, and a diffuse cancerization of the breast leaving no normal reference area in three cases. The patients' characteristics are given in Table 1.

2.4 CONTRAST EVALUATION

Contrast was evaluated for all imaging modalities comparing the tumor area with either one of two predefined reference areas, or with the entire breast map in craniocaudal view. The reference areas were selected by hand according to the following definitions:

Reference area 1: situated in the area of maximum breast thickness, as close as possible to the chest wall and to the center of the breast, but at a distance of at least one tumor diameter from the tumor area. The reference area is four times larger than the tumor area, as long as this is possible without violating any previous condition.

Reference area 2: situated at the same distance from the boundary as the tumor area. The reference area has the same size as the tumor area. If possible, the reference area is located symmetrical to the tumor with respect to the middle axis of the breast.

Table 1 Clinical characteristics of 20 breast cancer cases evaluated for contrast in FLM.

No.	Age	Max. diameter (mm)	TNM	Grading	Histol. type	Mammography
5	62	10	T1bN0M0	1	Ductal invasive	Spiculated mass
9	72	5	T1aN0M0	2	Ductal invasive, pred. intraductal	Smooth mass
10	55	30	T2N0M0	2	Ductal invasive	Smooth mass
15	47	30	T2N0M0	2	Ductal invasive, pred. intraductal	Smooth mass
22	46	22	T2N0M0	2	Mucinous	Smooth mass
27	55	15	T1cN0M0	3	Ductal invasive	Structural distortion
30	59	30	T2N0M0	3	Ductal invasive	Structural distortion
32	64	34	T2N0M0	1	Papillary	Spiculated mass
34	52	15	T1cN0M0	2	Ductal invasive	Smooth mass
36	54	16	T1cN0M0	1	Papillary	Spiculated mass
37	79	18	T1cNxM0	1	Papillary	Spiculated mass
38	55	25	T2N0M0	2	Medullary	Smooth mass
41	37	20	T1cN0M0	3	Ductal invasive	Structural distortion
42	55	80	T3N1M0	1	Apocrine	Spiculated mass
43	62	24	T2N1M0	2	Lobular invasive	Smooth mass
44	51	22	T2N0M0	3	Ductal invasive	Spiculated mass
51	39	18	T1cN1M0	1	Tubular	Spiculated mass
53	79	18	T4bNxM0	2	Ductal invasive	Microcalcifications
54	75	34	T2N1M0	1	Ductal invasive	Unsuspectious
59	52	18	T1cN0M0	3	Ductal invasive	Spiculated mass

2.4.1 Contrast Definitions

Definition 1: The first definition of contrast (C_1) is generally defined as

$$C_{1Tum,Ref} = \frac{\bar{S}_{Tum} - \bar{S}_{Ref}}{\bar{S}_{Ref}},$$

where \bar{S}_{Tum} (\bar{S}_{Ref}) is the average signal measured over the defined tumor (reference) area. This definition is not well suited for the comparison of different imaging algorithms, since the results depend on the absolute signal intensity and may be subject to systematic errors not reflecting true changes in subjective detectability of inhomogeneities. We thus have developed a second contrast definition (C_2) which relates differences to the noise of the signal measured in the supposedly normal breast area: contrast definition 2

$$C_{2Tum,Ref} = \frac{|\bar{S}_{Tum} - \bar{S}_{Ref}|}{\sigma(S_{Ref})},$$

where $\sigma(S_{Ref})$ is the standard deviation of the measured signal over the reference area as a measure of the image noise in the normal breast. This contrast definition should meet the subjective impression of contrast, if the reference area reflects the direct surrounding of a tumor. The overall detectability is best represented by choosing the entire breast area except the tumor area as the reference area. In this case $\sigma(S_{Ref})$ reflects the dynamic range of the entire data set.

However, both contrast definitions still are based on the assumption of a normal distribution of the data. They are prone to systematic errors, when comparing different mathematical algorithms, and are not well suited to determine whether the separation of tumor and normal breast data is improved or impaired by a particular algorithm. Thus we developed a third, nonparametric contrast definition which describes the probability that tumor and reference areas are in effect samples of different entities by means of the nonparametric Mann-Whitney-Wilcoxon U test. The test parameter U is

determined after ranking all pixel values of tumor and reference area together as

$$U_1 = n_{\text{ref}} \cdot n_{\text{tum}} + \frac{n_{\text{ref}}(n_{\text{ref}} + 1)}{2} - R_{\text{ref}},$$

$$U_2 = n_{\text{ref}} \cdot n_{\text{tum}} + \frac{n_{\text{tum}}(n_{\text{tum}} + 1)}{2} - R_{\text{tum}},$$

$$U = \text{Min}(U_1, U_2),$$

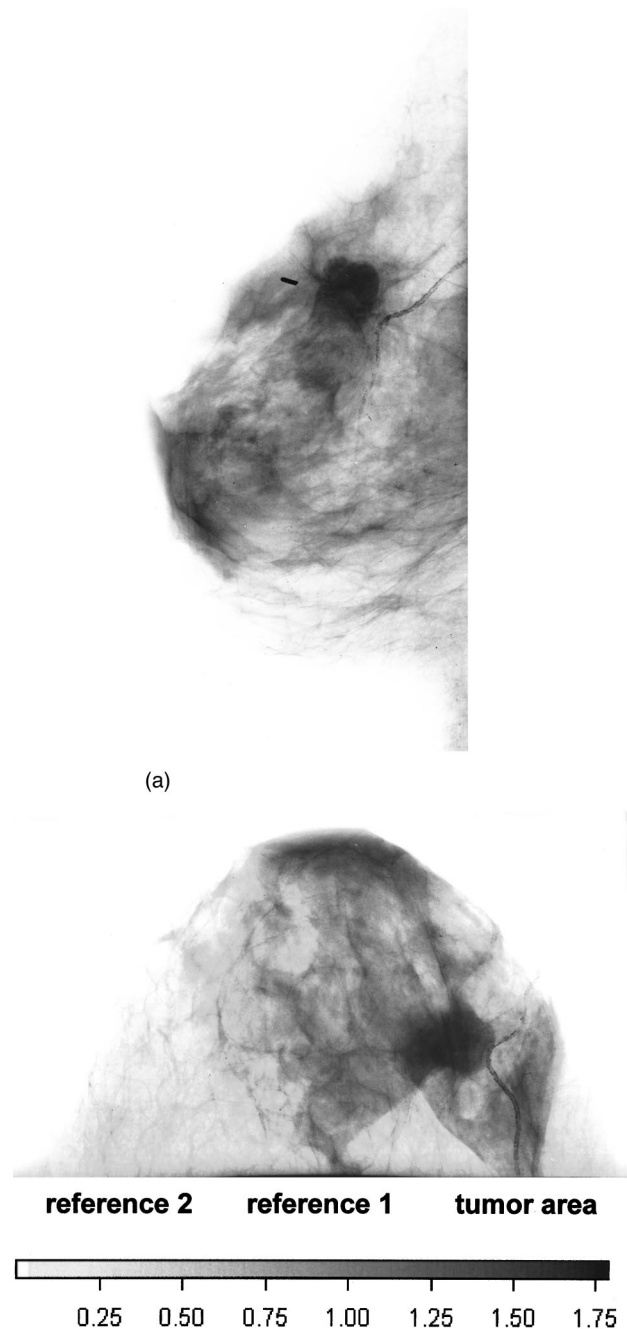
where n_{ref} denotes the number of pixels in the reference, n_{tum} the number of pixels in the tumor area, R_{ref} the sum of the ranks in the reference, and R_{tum} the sum of the ranks in the tumor area. According to the approximation of Mann and Whitney,¹³ for large n (>8), U for the two sided hypothesis can be translated into z of the normal distribution

$$\hat{z} = \frac{\left| U - \frac{n_{\text{ref}} \cdot n_{\text{tum}}}{2} \right|}{\sqrt{\frac{n_{\text{ref}} \cdot n_{\text{tum}}(n_{\text{ref}} + n_{\text{tum}} + 1)}{12}}}.$$

The higher z is, the better is the data separation, independently of absolute values and of the data distribution. This contrast definition fails, however, if no overlap exists in the data, since then, any quantitative improvement in the data separation will not be reflected by an improvement of z .

3 RESULTS

Figures 1(a) and 1(b) show the x-ray mammogram of a 16 mm diameter papillary cancer in the right outer upper quadrant of a 54 year old woman. The FLM images [N image, IR, linear gray scale, Figures 2(a) and 2(b)] show an increased mean data value in the area corresponding to the tumor location in both views. In correlating the geometrical position of the tumor found with x-ray mammography and FLM, one must take into account the different compression features and the loss of approximately 2 cm of breast tissue towards the chest wall in FLM. The tumor area and the two reference areas are marked in Figure 2(b) as defined in the materials section. Histograms of the amplitude data (Figure 3) reveal the large dynamic range and the asymmetry of the data distribution over the entire breast. The maximum of the curve represents the central area of the breast; the higher intensity values to the right reflect the higher transmission towards the boundaries. The reference area 1, by definition in the middle of the breast, corresponds to the data maximum. The reference area 2 is located more towards the boundary, and, thus, contains higher data values. The tumor area, which is geometrically located in a position comparable to the reference area 2 with respect to the breast boundary, contains



(b)

Fig. 1 X-ray mammogram of case No. 36: 54 year old woman presenting a 16 mm papillary cancer (pTlcNOMO) in the upper outer quadrant of her right breast. The mammographic appearance is classified "highly suspect." (a) Mediolateral view, (b) craniocaudal view.

the lowest values. The effect of a tumor on the transmission of near infrared light intensity by breast tissue is best represented by comparison with reference area 2. When comparing with the mean intensity collected on the entire breast, the contrast is falsely improved by the asymmetric data distribution.

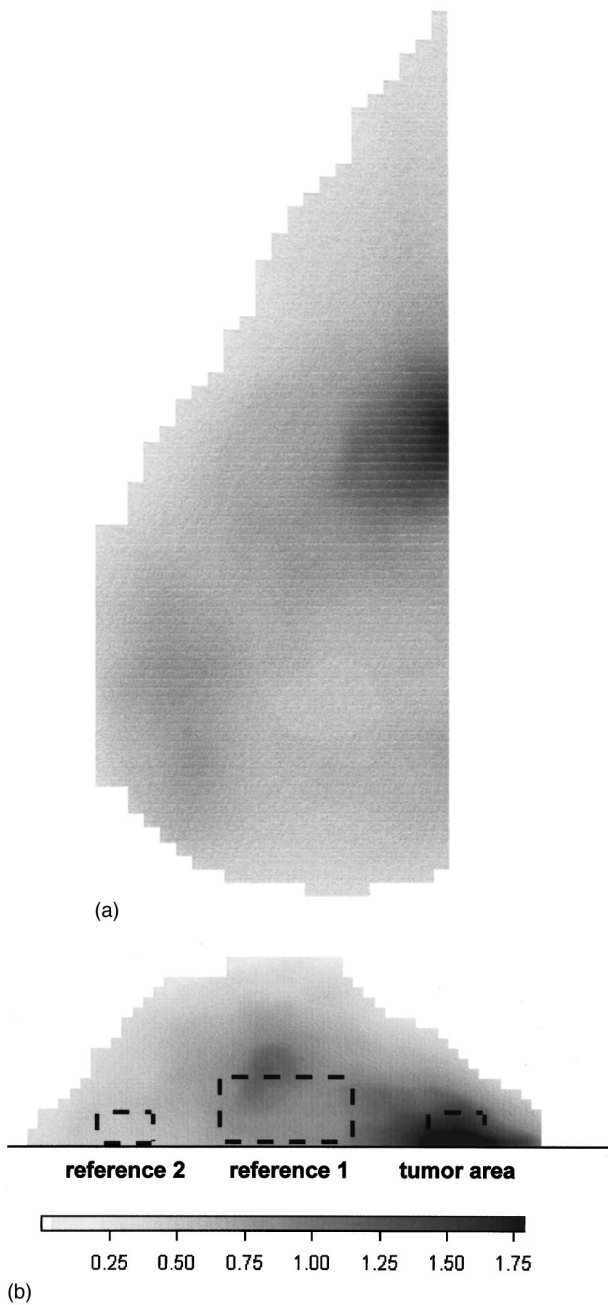


Fig. 2 Optical mammography (FLM) of case No. 36, image calculated from amplitude and phase signal at 810 nm, using the *N*-algorithm, linear gray scale. Comparing the tumor position with Figure 1, please refer to the different compression geometry as lined out in the text; (a) mediolateral view, (b) craniocaudal view. An example for the positioning of the tumor and reference areas is shown.

Figure 4 depicts the data distribution resulting from the *N* algorithm. The distribution is rather symmetric and centered around the value 0.8. The reference areas 1 and 2 show similar data. The strong geometric dependency has disappeared. The data over the tumor area is located towards the higher values of *N*, clearly outside the bulk of the breast data. Comparison with either one of the ref-

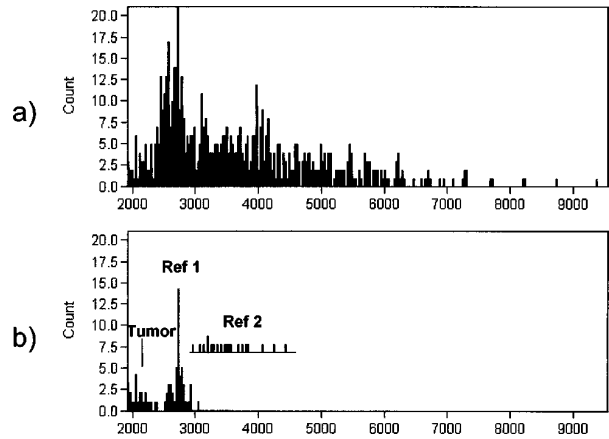


Fig. 3 Infrared amplitude data distribution (histogram) for case No. 36, craniocaudal view. The x axis reports the intensity (current) at the detector in arbitrary units. (a) Entire breast, (b) tumor and reference areas as shown in Figure 2.

erence areas or with the entire breast will yield similar results.

Forming the ratio between IR and Red amplitude signals (Figure 5), the overall data distribution is less asymmetric, too; reference areas 1 and 2 are more or less identical in their means. The tumor area, however, is now overlapping with the references. While the amplitude ratio effectively cancels the edge effects, it may cancel the tumor contrast, too.

For the 20 evaluated cancers, the quantitated contrast according to contrast definition 1 is given for reference areas 1, 2, and for the entire breast in Figure 6. As mentioned above for the individual case, in the raw data images (AC and Phase) the comparison with reference area 2 best reflects intrinsic optical changes due to the presence of a tumor. From Figure 6(b) it appears that such changes are minimal for the phase, while the AC signal shows a mean contrast of about 60% with respect to the reference area. Of course, being the phase predomi-

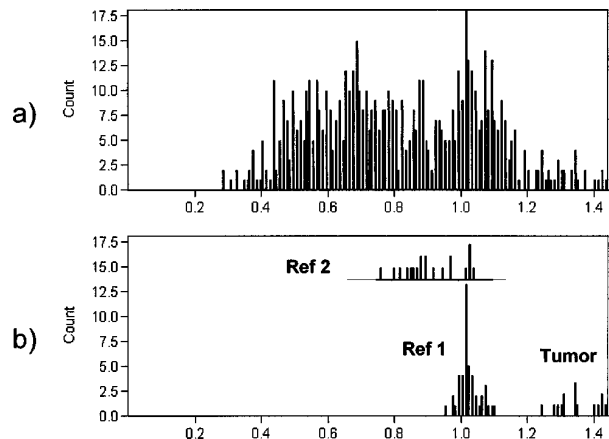


Fig. 4 *N*-value distribution for case No. 36, craniocaudal view. (a) Entire breast, (b) tumor and reference areas as shown in Figure 2.

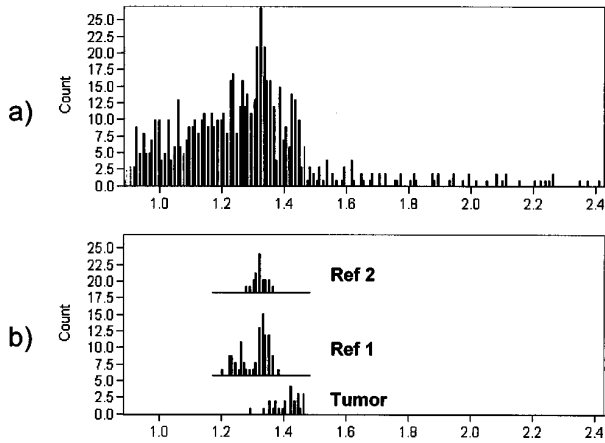


Fig. 5 Amplitude ratio infrared/red value distribution for case No. 36, craniocaudal view. (a) Entire breast, (b) tumor and reference areas as shown in Figure 2.

nantly influenced by the breast thickness, it gives relevant contrast when contrast is compared to reference areas with different mean breast thickness, by definition. The mean contrast values for the AC ratios or phase differences are lower than the con-

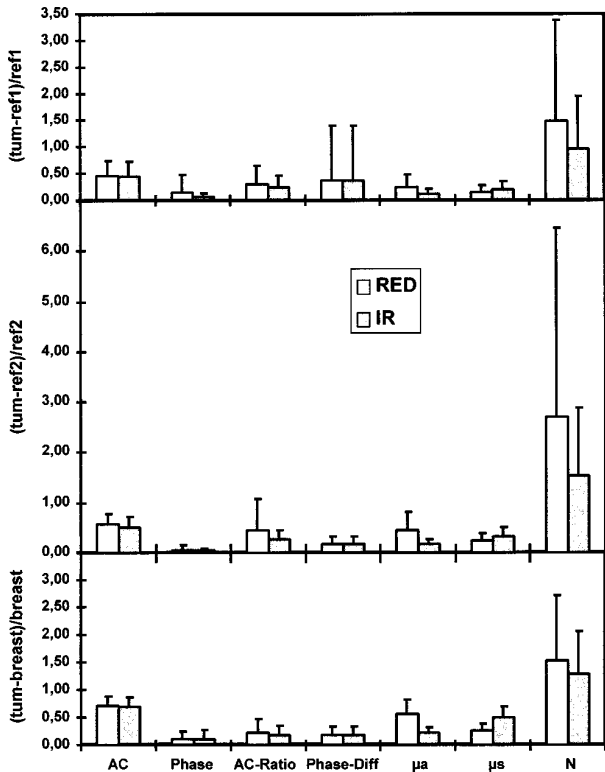


Fig. 6 Contrast calculated from contrast definition one ($C_{Tum,Ref} = |\bar{S}_{Tum} - \bar{S}_{Ref}| / \bar{S}_{Ref}$) for the comparison between tumor and reference areas 1 and 2, and between tumor and whole breast except tumor. (AC: amplitude image, Phase: phase image, AC Ratio: ratio between amplitude signals red/IR and IR/red, Phase-Diff: difference in phase red-IR or IR-red, μ_a : absorption coefficient μ_a as derived from amplitude and phase, μ_s : reduced scattering coefficient μ_s as determined from amplitude and phase N: parameter defined from an edge effect correction "flat-field" algorithm.)

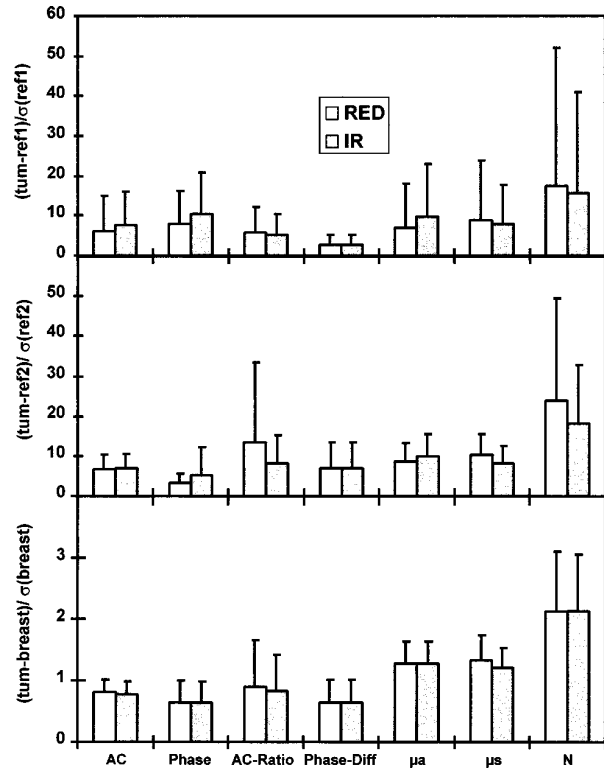


Fig. 7 Contrast calculated from contrast definition two ($C_{Tum,Ref} = |\bar{S}_{Tum} - \bar{S}_{Ref}| / \sigma(S_{Ref})$) for the comparison between tumor and reference areas 1 and 2, and between tumor and whole breast except tumor. (AC: amplitude image, Phase: phase image, AC Ratio: ratio between amplitude signals red/IR and IR/red, Phase-Diff: difference in phase red-IR or IR-red, μ_a : absorption coefficient μ_a as derived from amplitude and phase, μ_s : reduced scattering coefficient μ_s as determined from amplitude and phase, N: parameter defined from an edge effect correction "flat-field" algorithm.)

trast in AC at either wavelength, indicating little spectral differences between the optical properties of tumors and those of normal tissue. Again, in good agreement with the single case reported above, the calculated images ruling out the breast thickness using the phase information by one way or the other, give comparable contrasts with reference areas 1, 2, and with the entire breast area. The μ_a and μ_s images do not convey improved contrast over the AC contrast. The highest contrast is obtained by the N image, exceeding the AC value by at least a factor of 2.

The contrast resulting from contrast definition 2 (Figure 7) is an order of magnitude higher than that given by contrast definition 1, when the comparison is made with rather homogenous reference areas. It drops to levels similar to the contrast definition 1 if the entire breast is taken as the reference area. The phase signal now shows higher contrast, which reflects the little variation of the data within a reference area and underlines the potential significance of even small parameter changes. No significant improvement over the contrast in AC is obtained by any imaging modalities other than the N

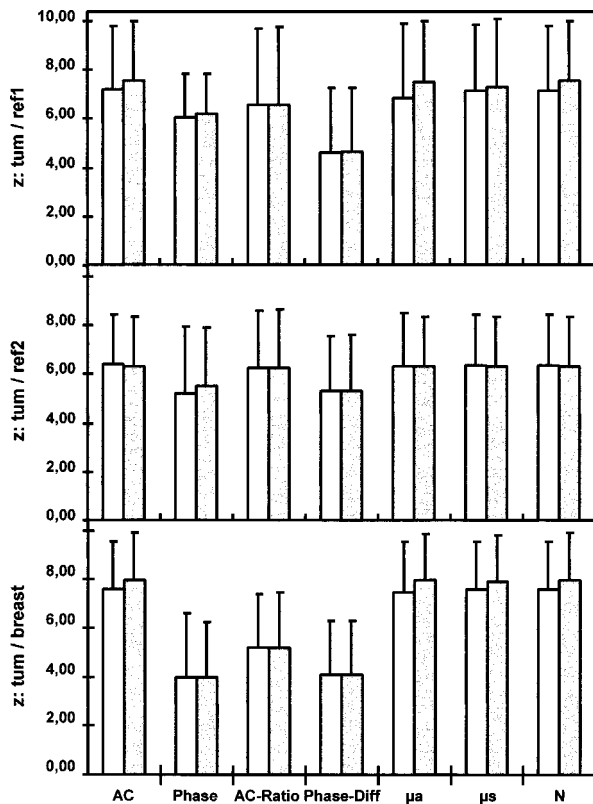


Fig. 8 Contrast as derived from nonparametric contrast definition 3 for the comparison between tumor and reference areas 1 and 2, and between tumor and whole breast except tumor. The tumor z represents the probability that tumor and reference area belong to the same global entity. The probability z is normally distributed, i.e., a value of $z=0$ means highest probability, higher values of z thus represent better contrast. [AC: amplitude image, Phase: phase image, AC Ratio: ratio between amplitude signals red/IR and IR/red, Phase-Diff: difference in phase red-IR or IR-red, μ_a : absorption coefficient μ_a as derived from amplitude and phase, μ_s : reduced scattering coefficient μ_s as determined from amplitude and phase, N : parameter defined from an edge effect correction "flat-field" algorithm (see Reference 11).]

image, when contrast is calculated between the tumor and the reference areas 1 or 2. The contrast with respect to the entire breast is slightly improved by the μ_a and μ_s algorithms. For all comparisons, the best contrast is obtained with the N algorithm.

The nonparametric contrast definition [Figures 8(a)–8(c)] reveals identical z values for AC, μ_a , μ_s , and N images. This is only partially due to the fact that some of the tumors do not present any overlap with the remainder of the breast data. While the phase signal does show nonparametric contrast, the combination of phase and AC information so far did not improve the data separation between the tumor area and the breast. However, the AC ratio and phase difference images show a worse separation between tumor and the entire breast, with respect to the AC image at either wavelength.

4 DISCUSSION

Due to the considerable geometrical difference between the compression pattern in FLM (minimal compression between parallel planes) and the one used by x-ray mammography (short duration, maximal compression between oblique planes), the tumor area cannot be located with sufficient precision by simple comparison with x-ray mammography. Thus, only tumors readily localizable in two perpendicular views of FLM were entered into the present study. The obvious bias resulting from the selection of visible, thus high contrast cases for the distribution of absolute values is canceled for the comparison between the imaging modalities, since we included all of those cases where the tumor area could be identified by any of the imaging algorithms. Since the benign lesions, with three exceptions, never gave an imaging correlate, a meaningful comparison with benign lesions was not possible or, one might say, is represented by the comparison with the reference areas.

The histograms of the raw data do reveal first of all the problem of imaging in a geometry with strong boundary effects. A large dynamic range in the amplitude signal results mainly from reduced thickness at the borders of the breast which is only partially compensated by photon losses at the boundary. This high dynamic range renders the imaging of small changes in absorption far from the boundary a difficult task, and close to the boundary an impossible one. Quantifying contrast by comparison with a centrally located reference area only partially reflects that problem by completely omitting the difficult edge areas. In the Swedish breast cancer transillumination trial, the problem of the boundary was solved by the use of a hand held light source, positioned manually against the breast in order to allow imaging by a video camera system.¹ By producing a number of different views, one would always bring a suspicious area to the center of the image, where boundary effects are negligible. The reproducibility of such investigation is, however, low and the sensitivity prone to considerable subjective influence. A sensitivity of 85% in the presence of clinical data thus dropped to 64% in the absence of such information. Since an advantage of the fixed geometry should be reproducibility, in order to get an objective description of the gain in overall imaging interpretability, we have represented a comparison between the tumor area with the entire breast area except the tumor, too. The latter demonstrates even better the improvement which is obtained by computing absorption with phase information. Of course, image formation from the amplitude ratio at the two wavelengths cancels the edge effects, too. However, it reduces the tumor contrast. This stands in contrast to the findings of a second group working in that field with an instrumentation using 70 MHz phase modulation, who found a sensitivity of 90% on a

single view basis, interpreting solely ratio images. However, they saw five times as many false positives than true positives, the ratio imaging approach being unable to differentiate between tumor and mastopathy. They communicated an attempt to analyze their data using the N -image algorithm as unsuccessful, obscuring their tumor images.¹⁴

Nevertheless, in our experience, the phase signal is the best way to flatten the amplitude signal field for geometric aberrations and thus to improve imaging of low contrast structural abnormalities on the basis of linear gray scales. The N -image algorithm did yield the best contrast results regardless of contrast definition and reference area.

However, the question arises whether there is an intrinsic and independent information by the phase signal with regard to tumor detection. To answer this question, we analyzed whether algorithms taking the phase signal into account did reduce the overlap between tumor and reference or between tumor and the entire breast area. The contrast definition chosen for this analysis is derived from non-parametric statistics and projects the overlap onto a normal distribution, thus enabling an intra- and inter-individual comparison. The contrast described in this way is now completely independent from data range and distribution characteristics and thus describes solely the amount of true differential information contained.

One conclusion of the minimal differences produced by this analysis can be that the phase signal does not carry *independent* information additionally differentiating the tumor from the normal tissue. This is somewhat intriguing, since from theory, absorption and scattering changes should differentially influence amplitude and phase signals, where the phase signal mainly carries the scattering information. Malignant tumors are expected to be differentiable predominantly by differences in their scattering rather than absorption properties.^{15,16} However, we did observe a very close correlation between μ_a and μ'_s , a fact which puts in doubt the correctness of the algorithms used. Alternatively, there may be a close link between absorption and scattering as a result of malignant transformation. On a logical basis, however, we prefer to think of a strong common influence of scattering and absorption on both amplitude and phase signals, combined with the incapability of our present technology and algorithms to effectively separate the two optical coefficients. We are still unable to specify whether the phase is just unnecessary to character-

ize the tumor optical properties or it may become a crucial parameter through more effective algorithms. For the moment, however, it serves best as a tool to correct for geometrical constraints of the instrumentation. Any additional parameter allowing to compensate the strong geometrical dependency of both amplitude and phase may still enable us to demonstrate an independent information by the phase signal.

This might seem somewhat deceiving, since we expected to get a substantial improvement in sensitivity by the intensity modulation. However, it should not be forgotten that by using the phase signal to correct for the difficult geometrical situation, a reproducible optical imaging, fairly independent from any subjective influences and manipulations, has been realized on a technological basis which gives ample room for further development.

Acknowledgments

We are grateful to E. Fischer-Funk, M.D. and C. Wetzel, M.D. for provision of and support in reading the x-ray mammographs. K.T.M. and S.T. acknowledge support from the Schott-Zeiss Foundation. S.F. and M.A.F. acknowledge support from Carl Zeiss for a work visit at Carl Zeiss, Oberkochen, Germany, and from the National Institutes of Health through Grant Nos. CA 57032 and RR10966-01.

REFERENCES

1. A. Alveryd, I. Andersson, K. Aspegren, G. Balldin, N. Bjurstaam, G. Edstrom, G. Fagerberg, U. Glas, O. Jarlman, and S. A. Larsson et al., "Lightscanning versus mammography for the detection of breast cancer in screening and clinical practice. A Swedish multicenter study," *Cancer* **65**, 1671-1677 (1990).
2. F. L. Greene, C. Hicks, V. Eddy, and C. Davis, "Mammography, sonomammography, and diaphanography (lightscanning). A prospective, comparative study with histologic correlation," *Am. Surg.* **51**, 58-60 (1985).
3. J. J. Gisvold, L. R. Brown, R. G. Swee, D. J. Raygor, N. Dickerson, and M. K. Ranfranz, "Comparison of mammography and transillumination light scanning in the detection of breast lesions," *AJR. Am. J. Roentgenol.* **147**, 191-194 (1986).
4. G. E. Geslien, J. R. Fisher, and C. DeLaney, "Transillumination in breast cancer detection: screening failures and potential," *AJR. Am. J. Roentgenol.* **144**, 619-622 (1985).
5. P. He, M. Kaneko, M. Takai, K. Baba, Y. Yamashita, and K. Ohta, "Breast cancer diagnosis by laser transmission photo-scanning with spectro-analysis (report 4)," *Radiat. Med.* **8**, 1-5 (1990).
6. O. Jarlman, I. Andersson, G. Balldin, and S. A. Larsson, "Diagnostic accuracy of lightscanning and mammography in women with dense breasts," *Acta Radiol.* **33**, 69-71 (1992).
7. E. B. de Haller and C. Depeursinge, "Simulation of time-resolved breast transillumination," *Med. Biol. Eng. Comput.* **31**, 165-170 (1993).